$$P_{\rm CDM}(k) \propto \frac{k^n}{\left[1 + 3.89q + (16.1q)^2 + (5.46q)^3 + (6.71q)^4\right]^{1/2}} \times \frac{\left[\ln\left(1 + 2.34q\right)\right]^2}{(2.34q)^2} \tag{13}$$

$$q = k/\Gamma$$

$$\Gamma = \Omega_{m,\circ} h \exp\left\{-\Omega_b - \frac{\Omega_b}{\Omega_{m,\circ}}\right\}$$

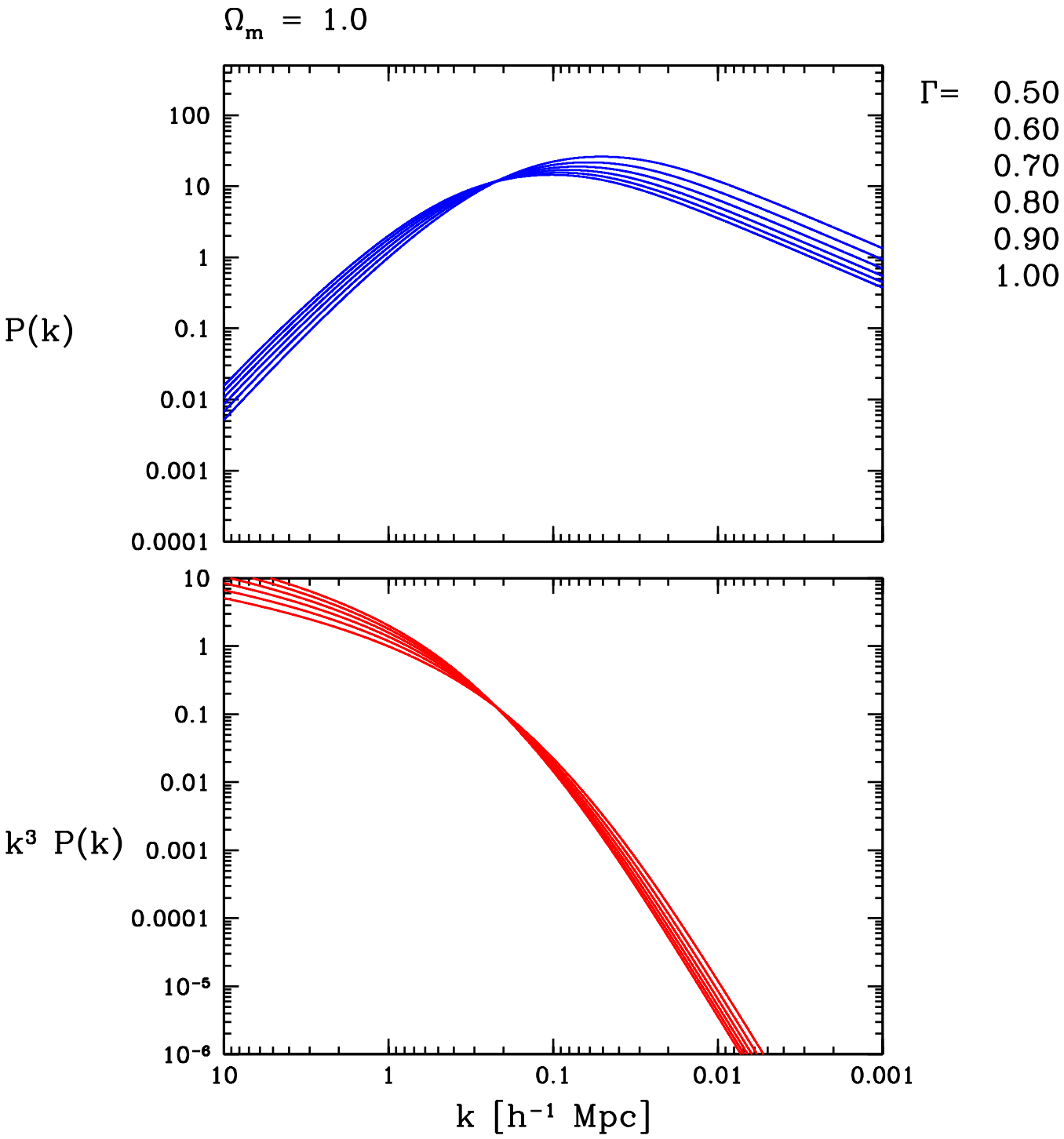
Ω_m = 1.0
Γ= 0.50
0.60
0.70
0.80
0.90
1.00
P(k)
100
10
1
0.1
0.01
0.001
0.0001
k^3 P(k)
10
1
0.1
0.01
0.001
0.0001
10^{-5}
10^{-6}
10
1
0.1
0.01
0.001
k [h^{-1} Mpc]

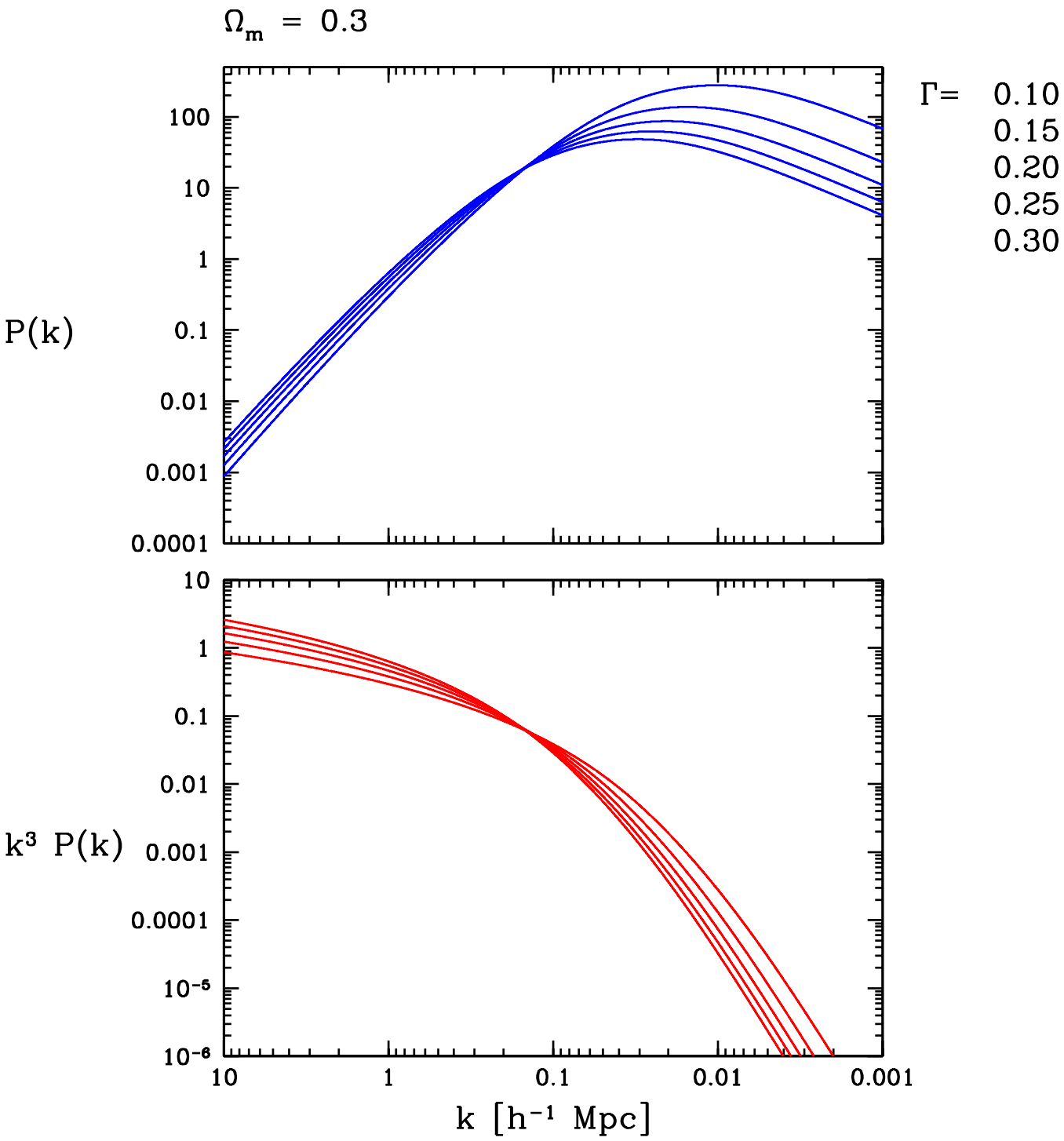
Ω_m = 0.3
Γ= 0.10
0.15
0.20
0.25
0.30
P(k)
100
10
1
0.1
0.01
0.001
0.0001
k^3 P(k)
10
1
0.1
0.01
0.001
0.0001
10^{-5}
10^{-6}
10
1
0.1
0.01
0.001
k [h^{-1} Mpc]

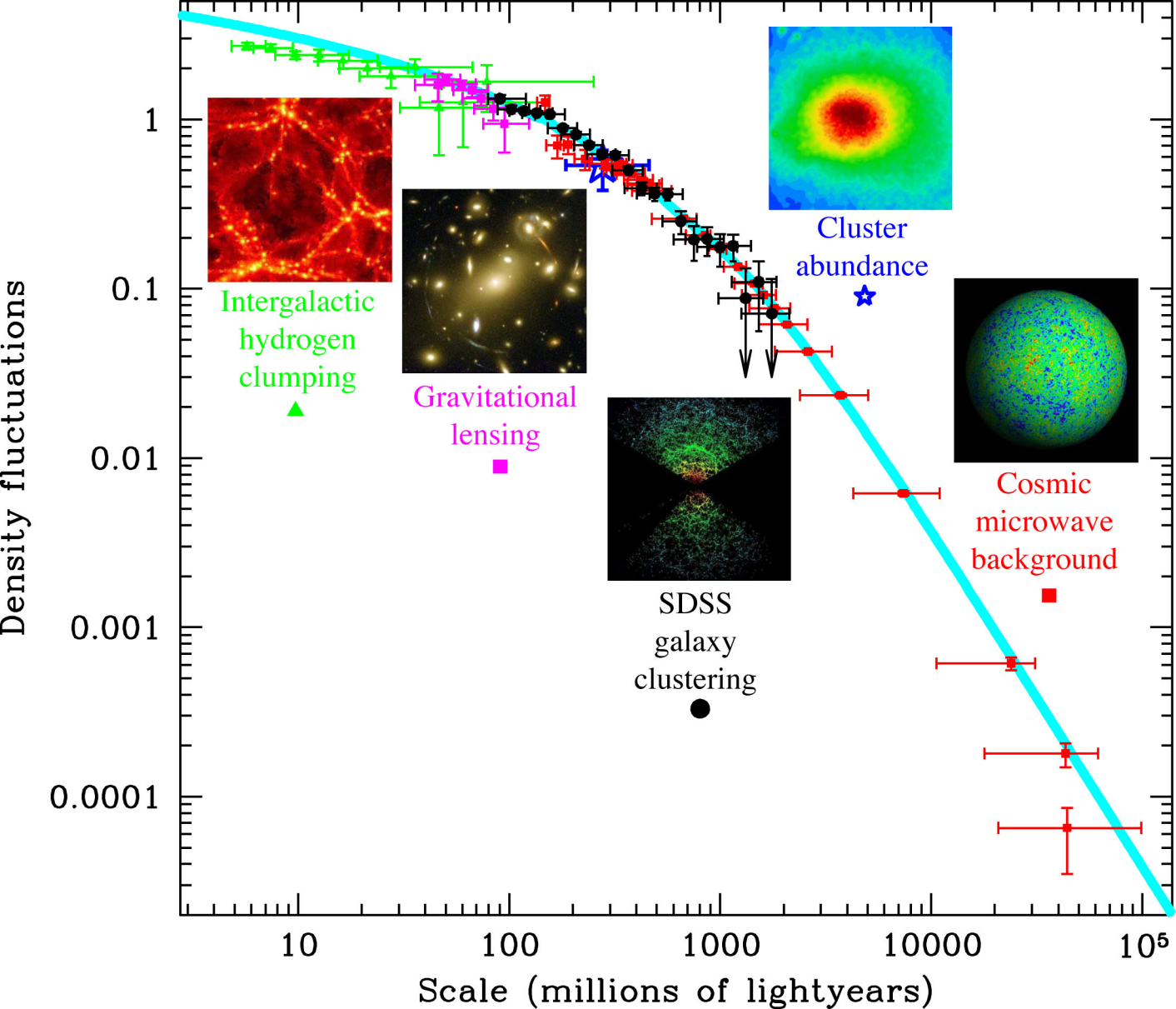
Density fluctuations
1
0.1
0.01
0.001
0.0001
10
100
1000
10000
10^5
Scale (millions of lightyears)
Intergalactic hydrogen clumping
Gravitational lensing
SDSS galaxy clustering
Cluster abundance
Cosmic microwave background

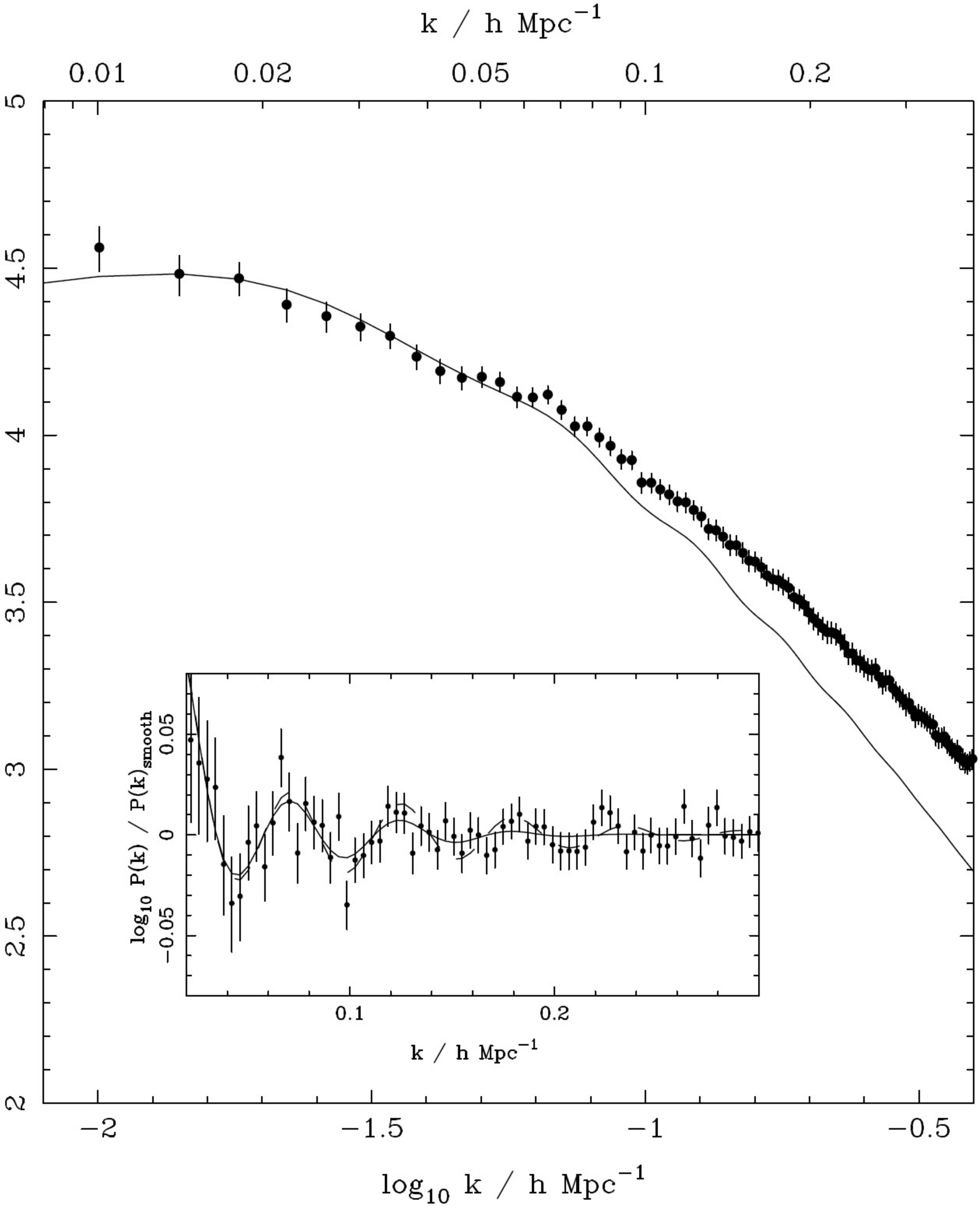
k / h Mpc^{-1}
0.01
0.02
0.05
0.1
0.2
log$_{10}$ P(k) / h^{-3}Mpc^3
5
4.5
4
3.5
3
2.5
2
log$_{10}$ P(k) / P(k)$_{smooth}$
0.05
0
−0.05
0.1
0.2
k / h Mpc^{-1}
−2
−1.5
−1
−0.5
log$_{10}$ k / h Mpc^{-1}

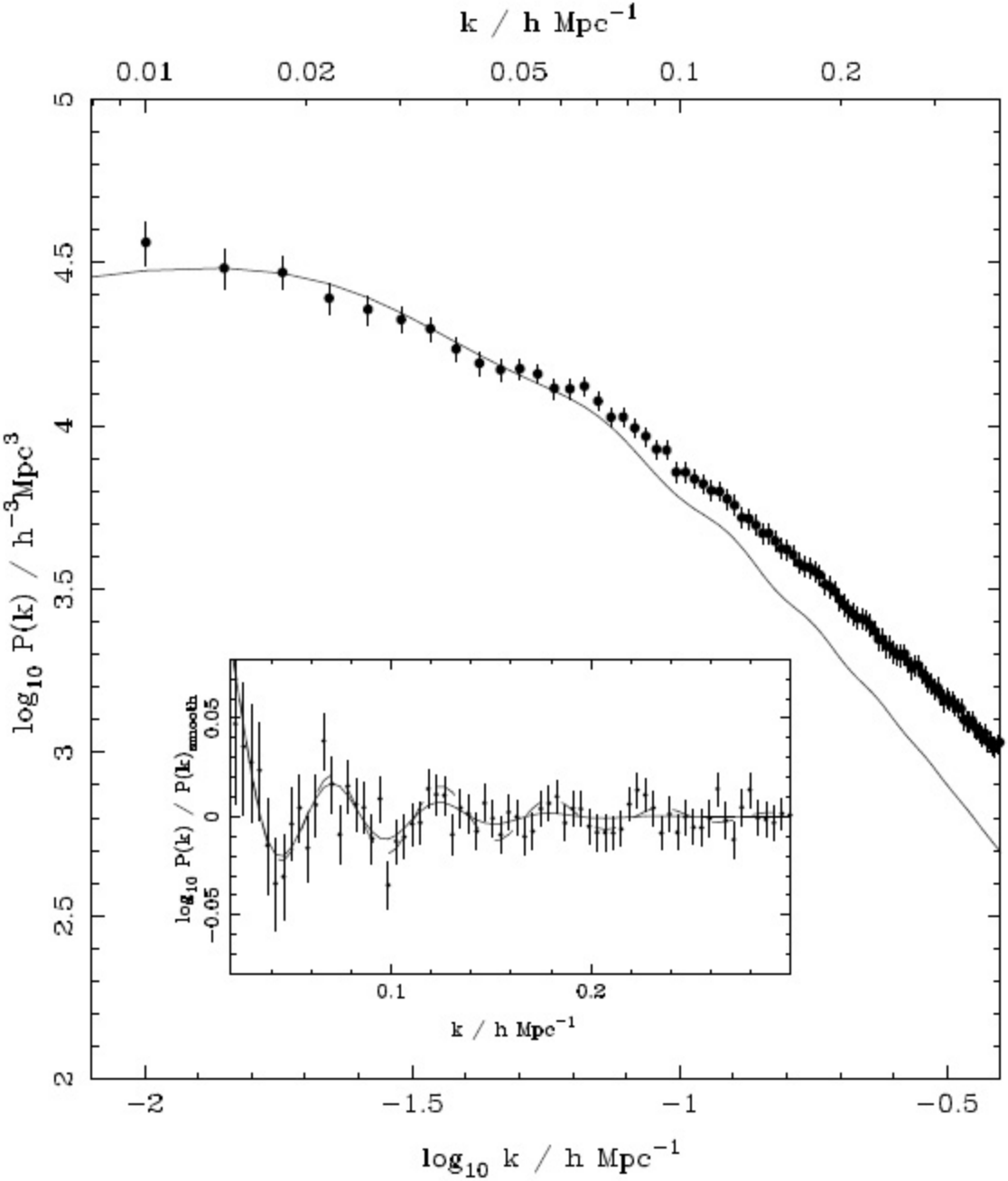

FIG. 12.— The redshift-space power spectrum recovered from the combined SDSS main galaxy and LRG sample, optimally weighted for both density changes and luminosity dependent bias (solid circles with 1-σ errors). A flat Λ cosmological distance model was assumed with $\Omega_M = 0.24$. Error bars are derived from the diagonal elements of the covariance matrix calculated from 2000 log-normal catalogues created for this cosmological distance model, but with a power spectrum amplitude and shape matched to that observed (see text for details). The data are correlated, and the width of the correlations is presented in Fig. 10 (the correlation between data points drops to < 0.33 for $\Delta k > 0.01\,h\,\mathrm{Mpc}^{-1}$). The correlations are smaller than the oscillatory features observed in the recovered power spectrum. For comparison we plot the model power spectrum (solid line) calculated using the fitting formulae of Eisenstein & Hu (1998); Eisenstein et al. (2006), for the best fit parameters calculated by fitting the WMAP 3-year temperature and polarisation data, $h = 0.73$, $\Omega_M = 0.24$, $n_s = 0.96$ and $\Omega_b/\Omega_M = 0.174$ (Spergel et al. 2006). The model power spectrum has been convolved with the appropriate window function to match the measured data, and the normalisation has been matched to that of the large-scale ($0.01 < k < 0.06\,h\,\mathrm{Mpc}^{-1}$) data. The deviation from this low Ω_M linear power spectrum is clearly visible at $k \gtrsim 0.06\,h\,\mathrm{Mpc}^{-1}$, and will be discussed further in Section 6. The solid circles with 1σ errors in the inset show the power spectrum ratioed to a smooth model (calculated using a cubic spline fit as described in Percival et al. 2006) compared to the baryon oscillations in the (WMAP 3-year parameter) model (solid line), and shows good agreement. The calculation of the matter density from these oscillations will be considered in a separate paper (Percival et al. 2006). The dashed line shows the same model without the correction for the damping effect of small-scale structure growth of Eisenstein et al. (2006). It is worth noting that this model is not a fit to the data, but a prediction from the CMB experiment.

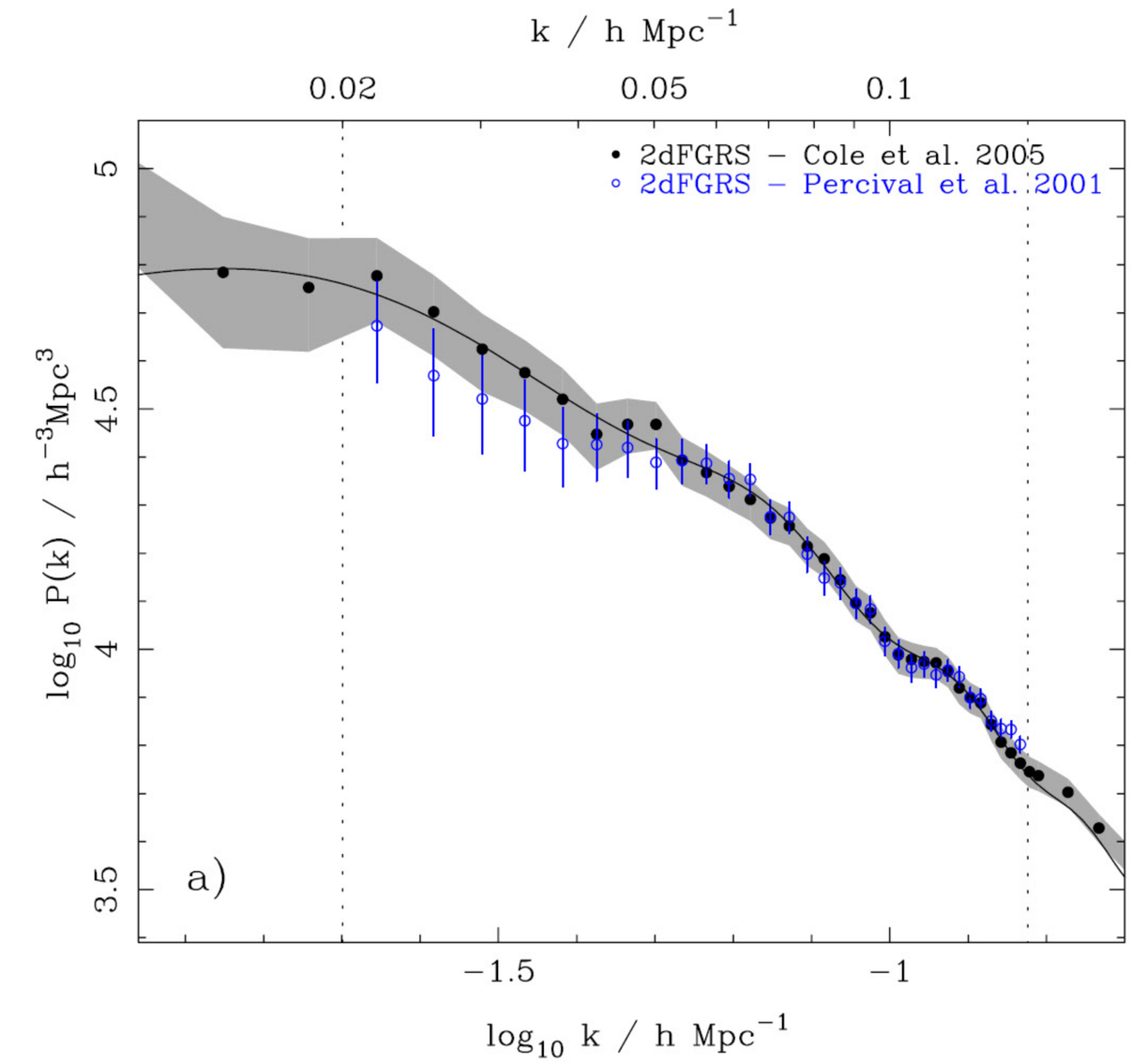
k / h Mpc^{-1}
0.02
0.05
0.1
• 2dFGRS – Cole et al. 2005
◦ 2dFGRS – Percival et al. 2001
log$_{10}$ P(k) / h^{-3}Mpc^3
5
4.5
4
3.5
a)
−1.5
−1
log$_{10}$ k / h Mpc^{-1}

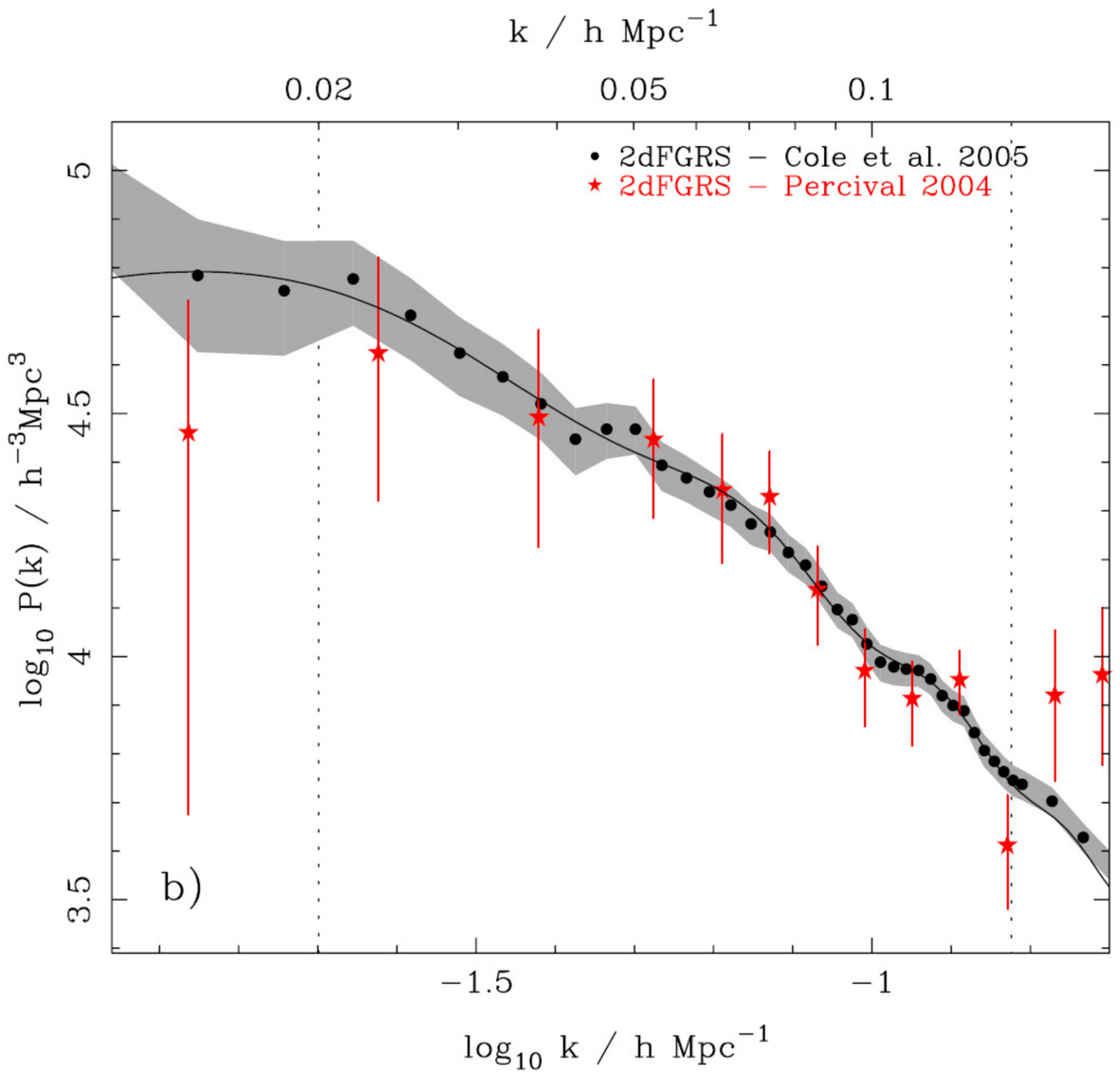
k / h Mpc^{-1}
0.02
0.05
0.1
• 2dFGRS – Cole et al. 2005
⋆ 2dFGRS – Percival 2004
log$_{10}$ P(k) / h^{-3}Mpc^3
5
4.5
4
3.5
b)
−1.5
−1
log$_{10}$ k / h Mpc^{-1}

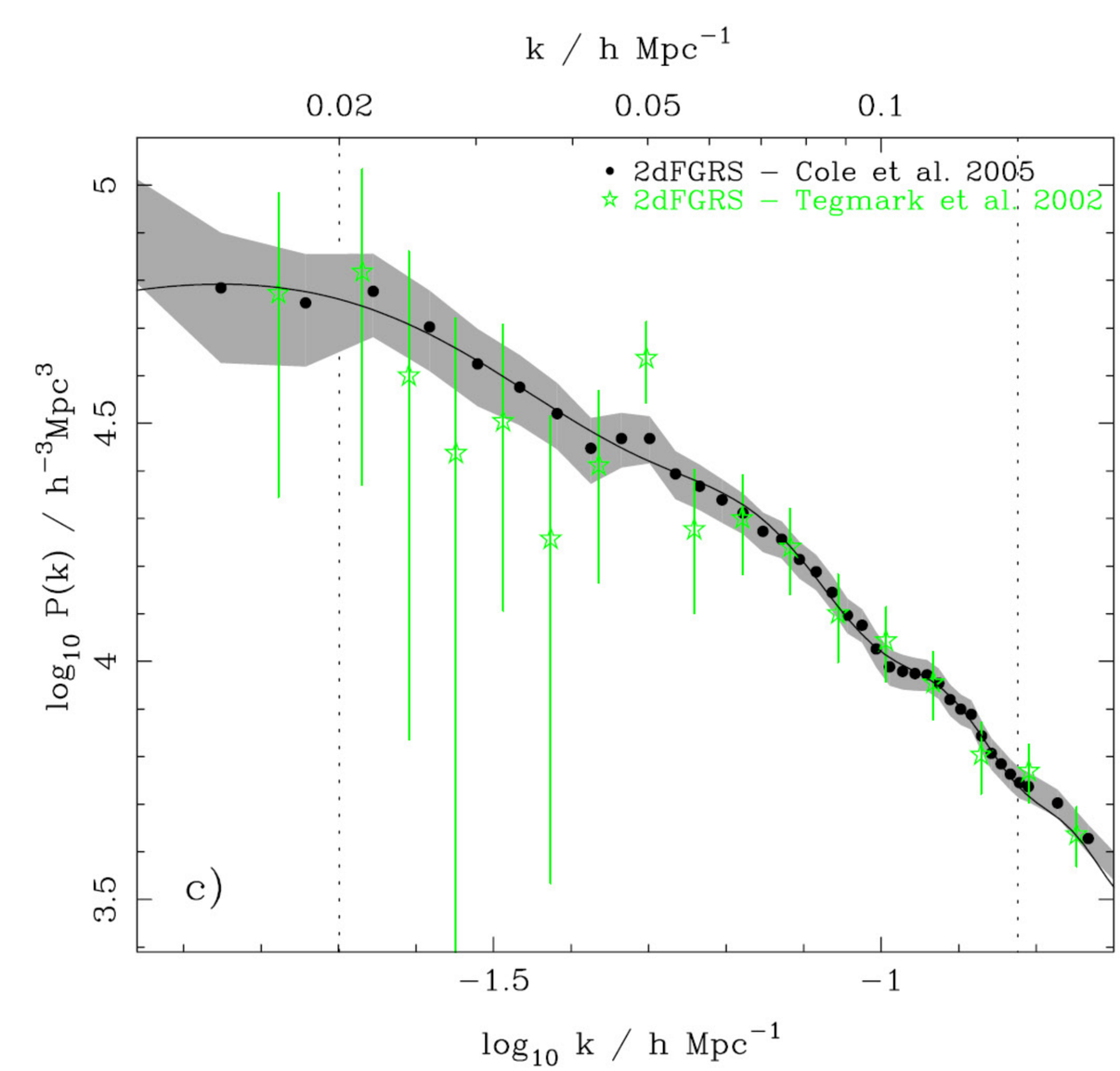
k / h Mpc^{-1}
0.02
0.05
0.1
• 2dFGRS – Cole et al. 2005
☆ 2dFGRS – Tegmark et al. 2002
log$_{10}$ P(k) / h^{-3}Mpc^3
5
4.5
4
3.5
c)
−1.5
−1
log$_{10}$ k / h Mpc^{-1}

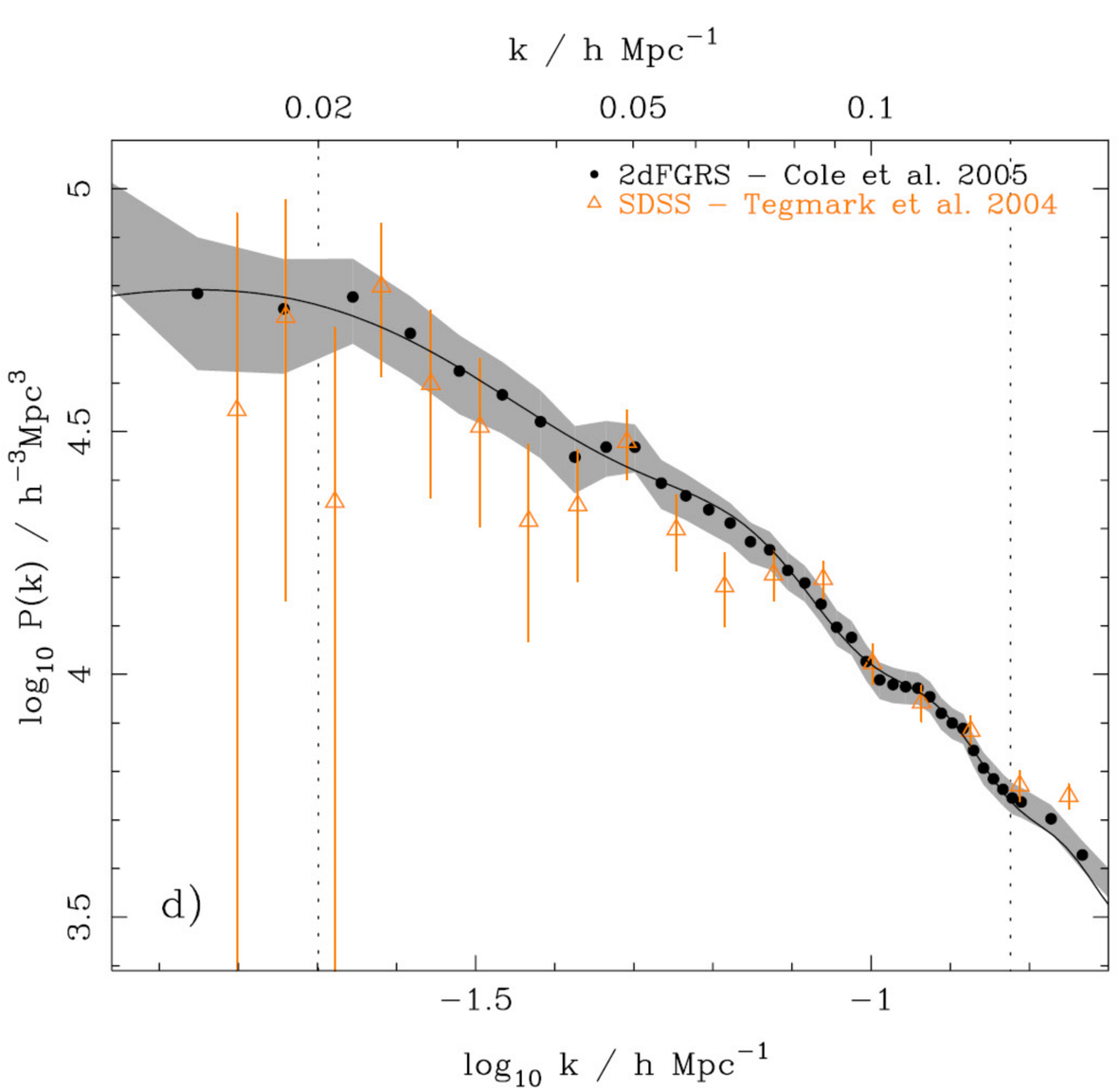
k / h Mpc^{-1}
0.02
0.05
0.1
• 2dFGRS – Cole et al. 2005
△ SDSS – Tegmark et al. 2004
log$_{10}$ P(k) / h^{-3}Mpc^3
5
4.5
4
3.5
d)
−1.5
−1
log$_{10}$ k / h Mpc^{-1}

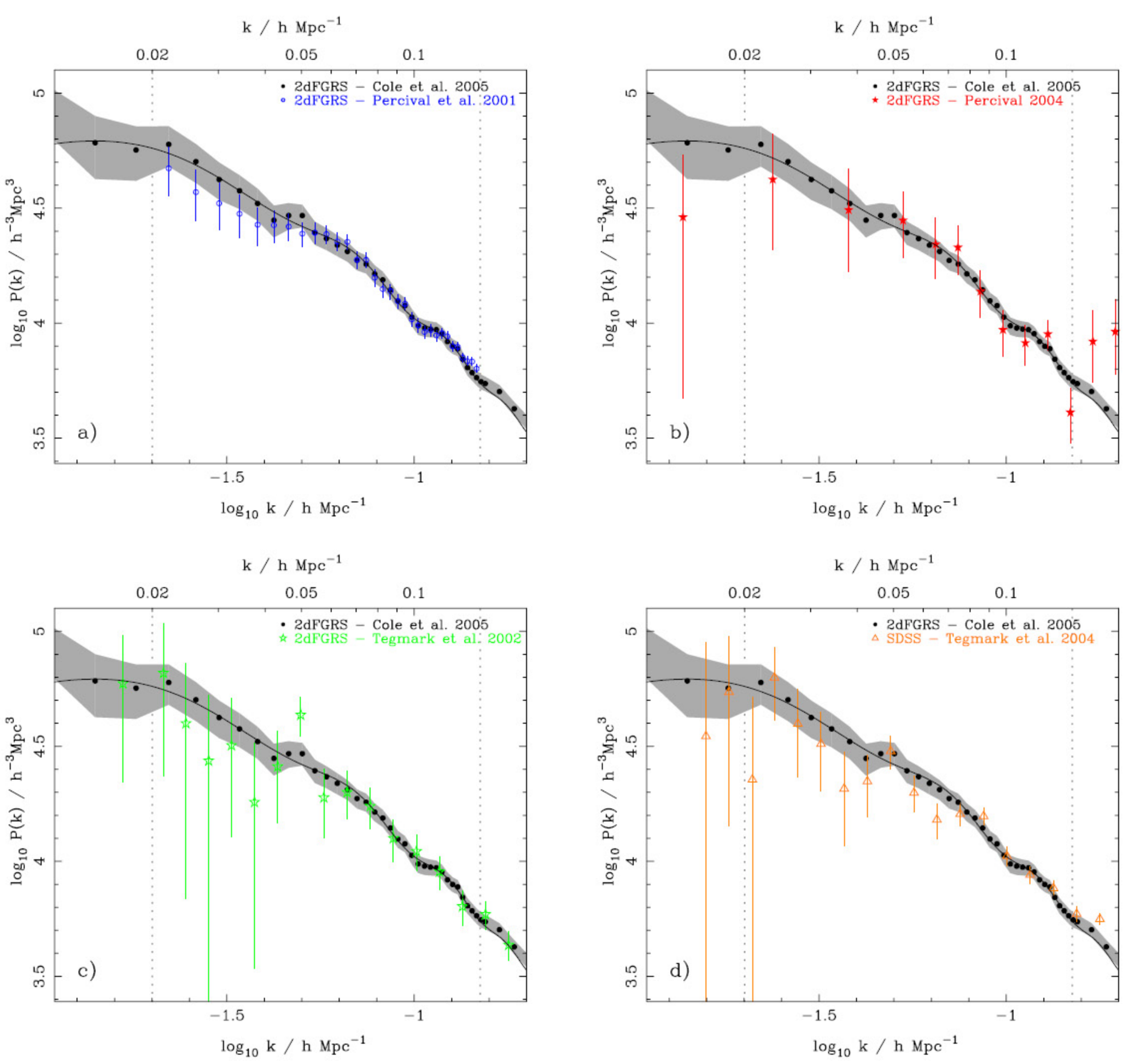

Figure 16. The redshift-space power spectrum calculated in this paper (solid circles with 1σ errors shown by the shaded region) compared with other measurements of the 2dFGRS power-spectrum shape by (a) Percival et al. (2001), (b) Percival (2005), and (c) Tegmark et al. (2002). For the data with window functions, the effect of the window has been approximately corrected by multiplying by the net effect of the window on a model power spectrum with $\Omega_{\rm m}h = 0.168$, $\Omega_{\rm b}/\Omega_{\rm m} = 0.0$, $h = 0.72$ & $n_{\rm s} = 1$. A zero-baryon model was chosen in order to avoid adding features into the power spectrum. All of the data are renormalized to match the new measurements. Panel (d) shows the uncorrelated SDSS real-space $P(k)$ estimate of Tegmark et al. (2004), calculated using their 'modelling method' with no FOG compression (their Table 3). These data have been corrected for the SDSS window as described above for the 2dFGRS data. The solid line shows a model linear power spectrum with $\Omega_{\rm m}h = 0.168$, $\Omega_{\rm b}/\Omega_{\rm m} = 0.17$, $h = 0.72$, $n_{\rm s} = 1$ and normalization matched to the 2dFGRS power spectrum.

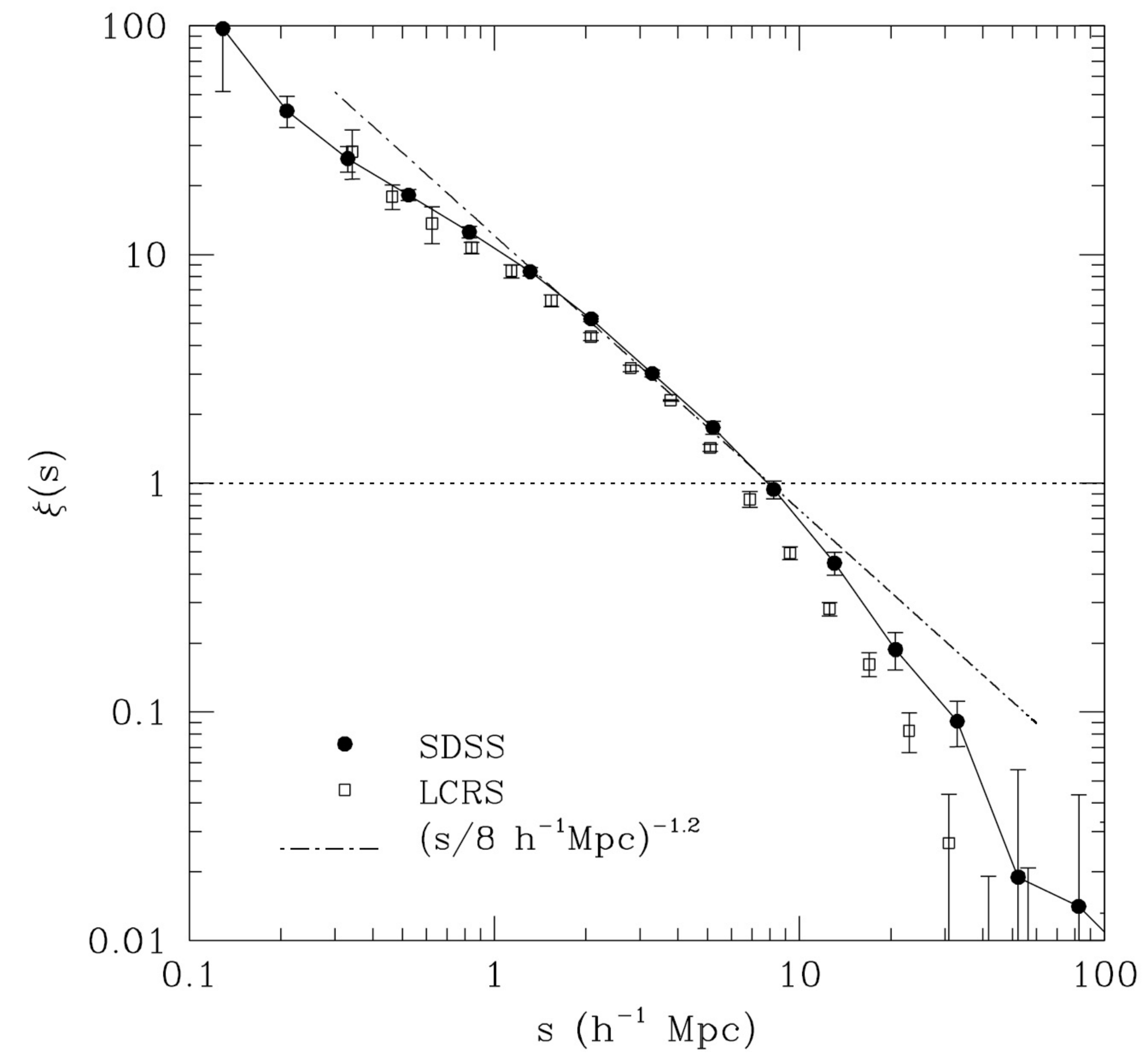
100
10
1
0.1
0.01
0.1
1
10
100
ξ(s)
s (h^{-1} Mpc)
SDSS
LCRS
(s/8 h^{-1}Mpc)$^{-1.2}$

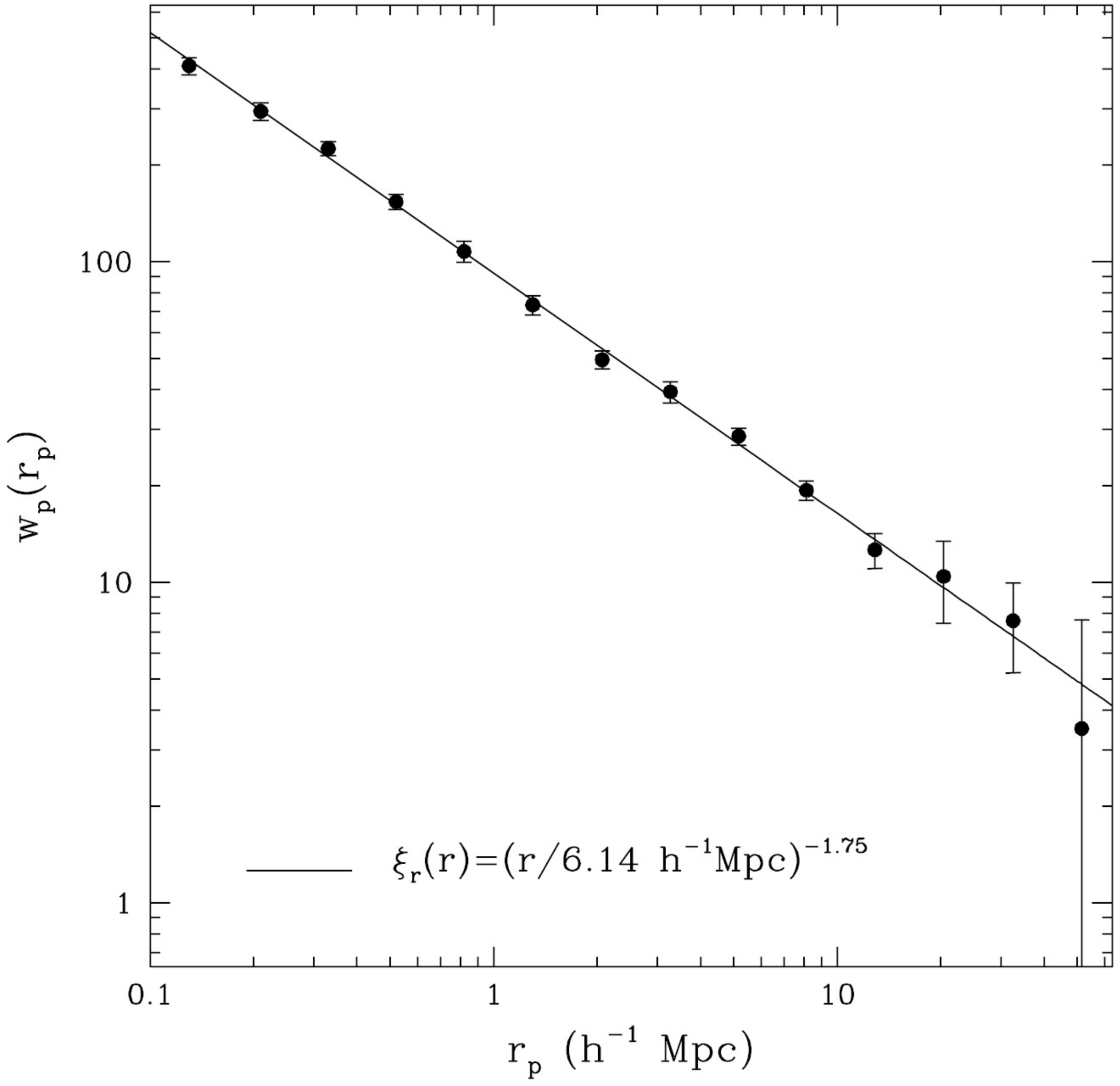
100
10
1
0.1
1
10
$W_p(r_p)$
$\xi_r(r)=(r/6.14\ h^{-1}Mpc)^{-1.75}$
$r_p\ (h^{-1}\ Mpc)$

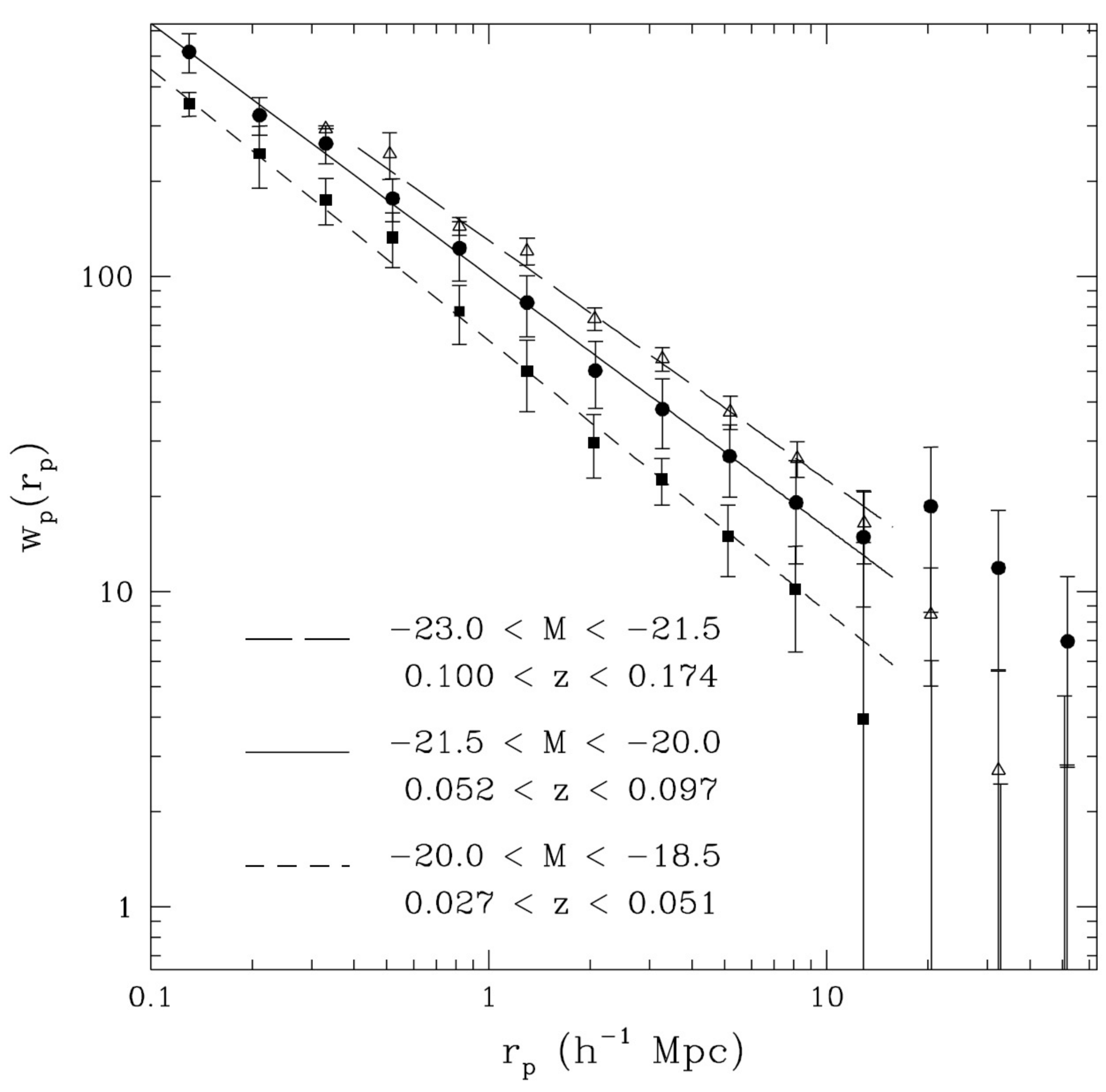
100
10
1
0.1
1
10
$w_p(r_p)$
r_p (h^{-1} Mpc)
−23.0 < M < −21.5
0.100 < z < 0.174
−21.5 < M < −20.0
0.052 < z < 0.097
−20.0 < M < −18.5
0.027 < z < 0.051

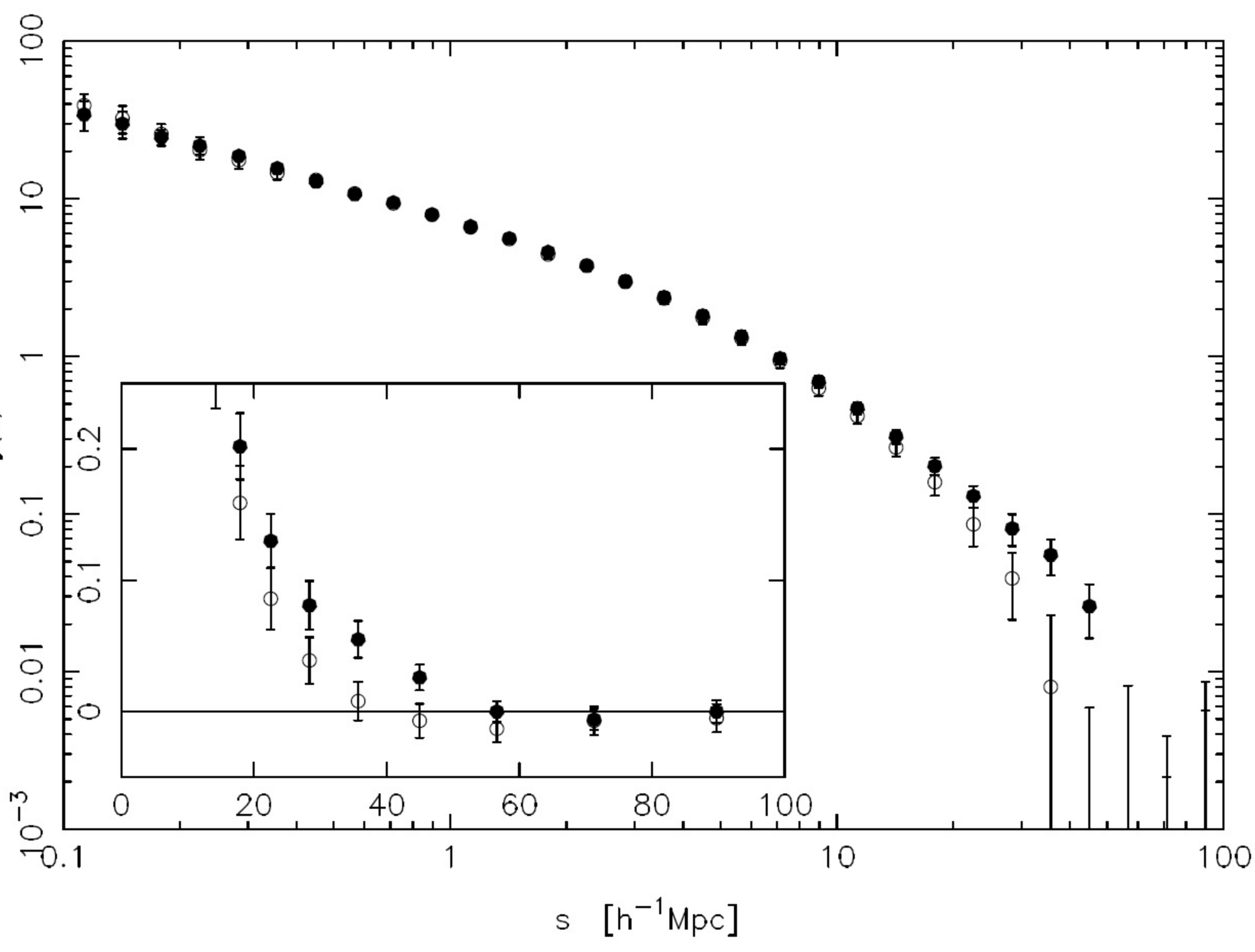
$\xi(s)$
10^{-3}
0.01
0.1
1
10
100
0.1
1
10
100
0
0.1
0.2
0
20
40
60
80
100
s [h^{-1}Mpc]

$\xi(s)$

100
10
1
0.01
0.1
0.2
0
0
20
40
60
80
100

$\xi_{data}/\xi_{power\ law}$

0
0.5
1
1.5

0.1
1
10
100

s $[h^{-1}Mpc]$

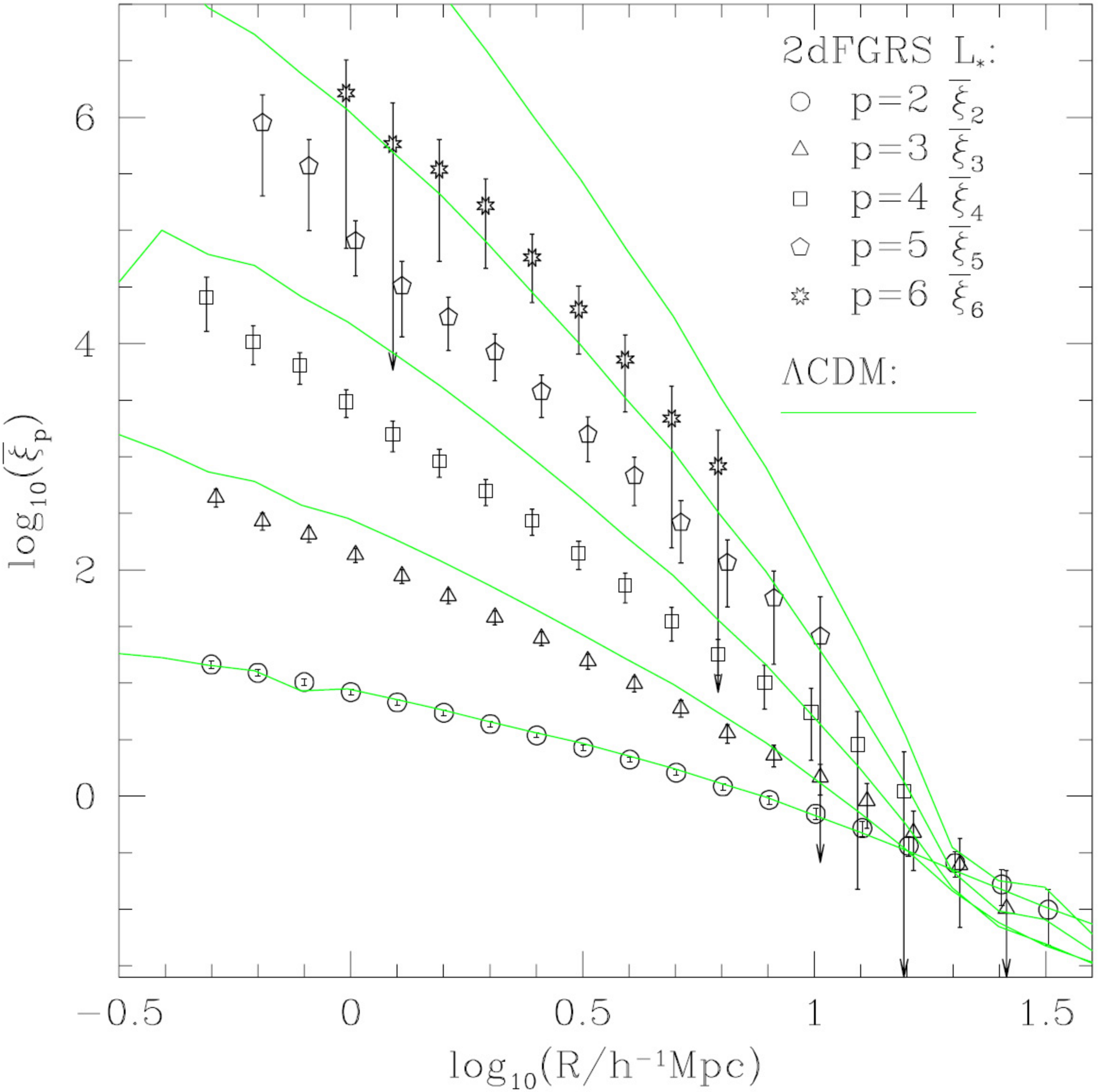
2dFGRS L*:
p=2 ξ̄2
p=3 ξ̄3
p=4 ξ̄4
p=5 ξ̄5
p=6 ξ̄6
ΛCDM:
log10(ξ̄p)
log10(R/h−1Mpc)
6
4
2
0
−0.5
0
0.5
1
1.5

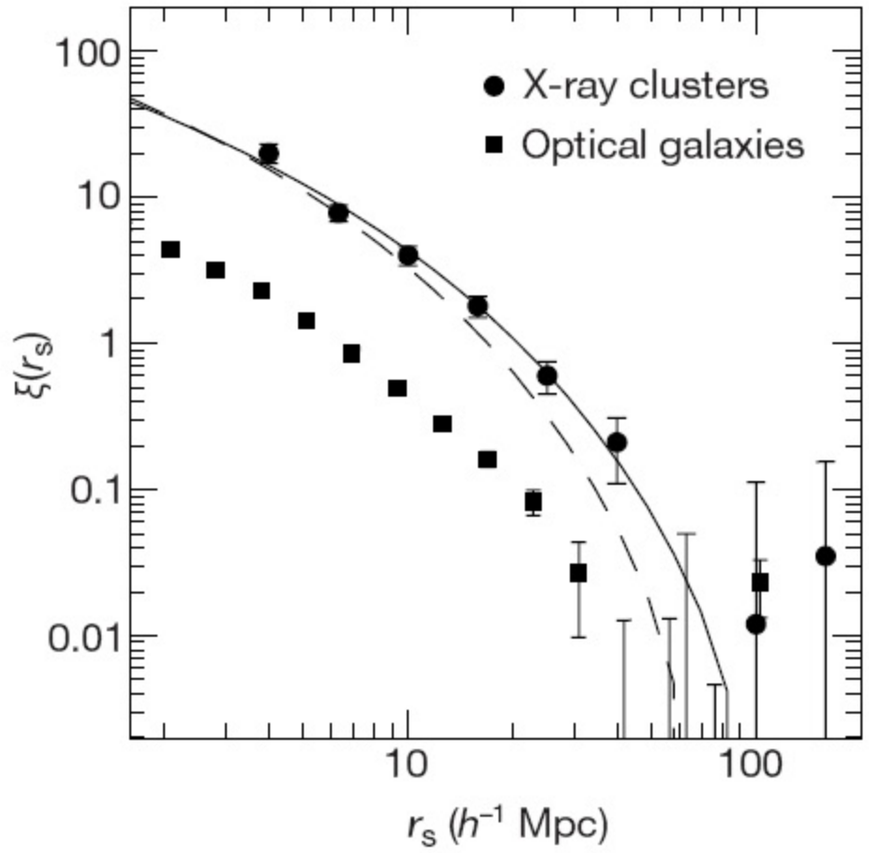

Figure 2 Statistical description of clustering. The two-point correlation functions ξ of galaxies (squares) and X-ray clusters of galaxies (circles), computed from the two data sets of Fig. 1[21,31], plotted as a function of separation r_s (where the subscript s indicates that all object distances are computed from the measured redshift). The curves are the predictions of two CDM models, with different density parameters Ω_m, for an X-ray cluster survey with the same flux limit as the real data. Solid curve: $\Omega_m = 0.3$ and Hubble parameter $h = 0.7$; dashed curve: $\Omega_m = 0.5$ and $h = 0.6$. Both models have flat spatial geometry provided by a cosmological constant contribution (that is, $\Omega_m + \Omega_\Lambda = 1$) and power-spectrum normalization chosen so as to be consistent with measured CMB anisotropies[15,16,64]. Also, we take $\Omega_{bar}h^2 = 0.019$ for the baryon density[79].

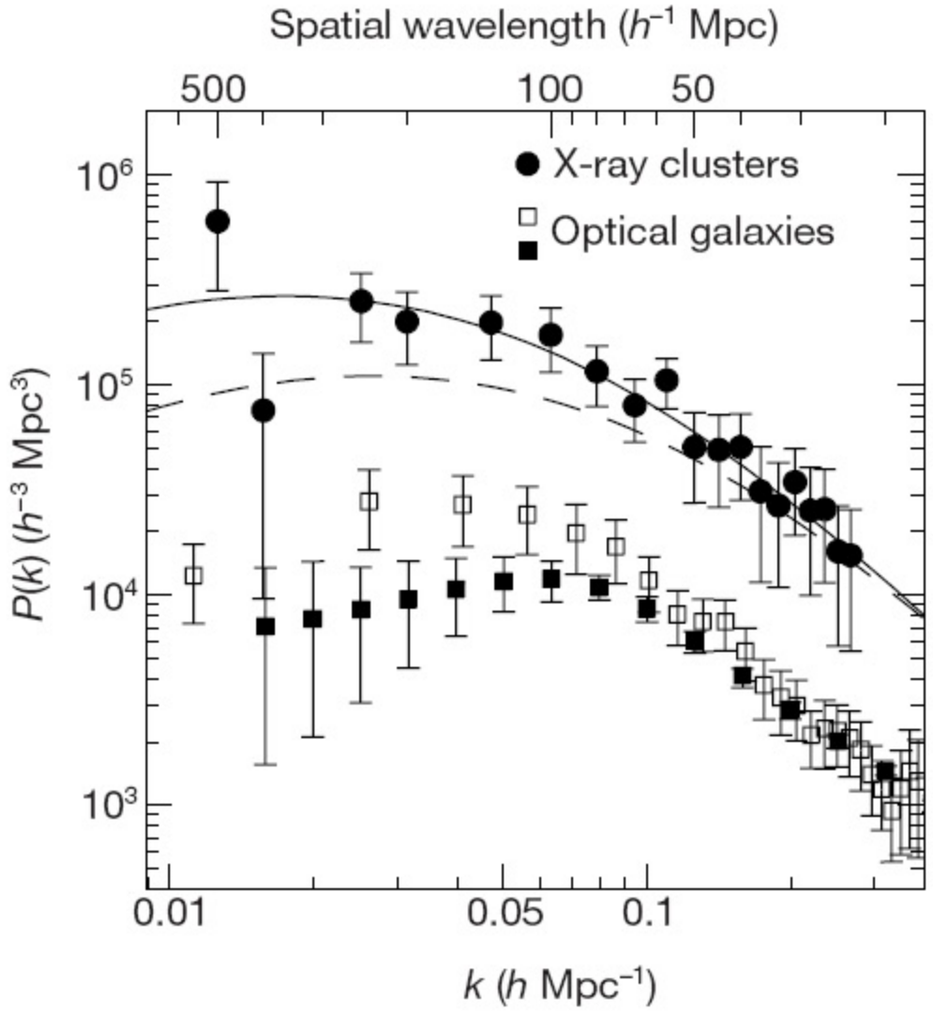

Figure 3 The power spectrum of the distribution of galaxies and X-ray clusters of galaxies from the data of Fig. 1. The squares are from galaxy data, which in addition to the LCRS points (filled squares[80]) include a measure from another survey with better volume coverage (open squares[81]). The filled circles show an estimate of the power spectrum of X-ray selected clusters from the REFLEX survey[32]. We note the rather different amplitude between the galaxy and cluster power spectra, similarly to that shown by correlation functions (see Fig. 2). The two curves are theoretical predictions from the same cosmological models shown in Fig. 2.

X-ray Clusters

Optical Galaxies

100

10

1

0.1

0.01

$\xi(r_s)$

10

100

r_s (h^{-1} Mpc)

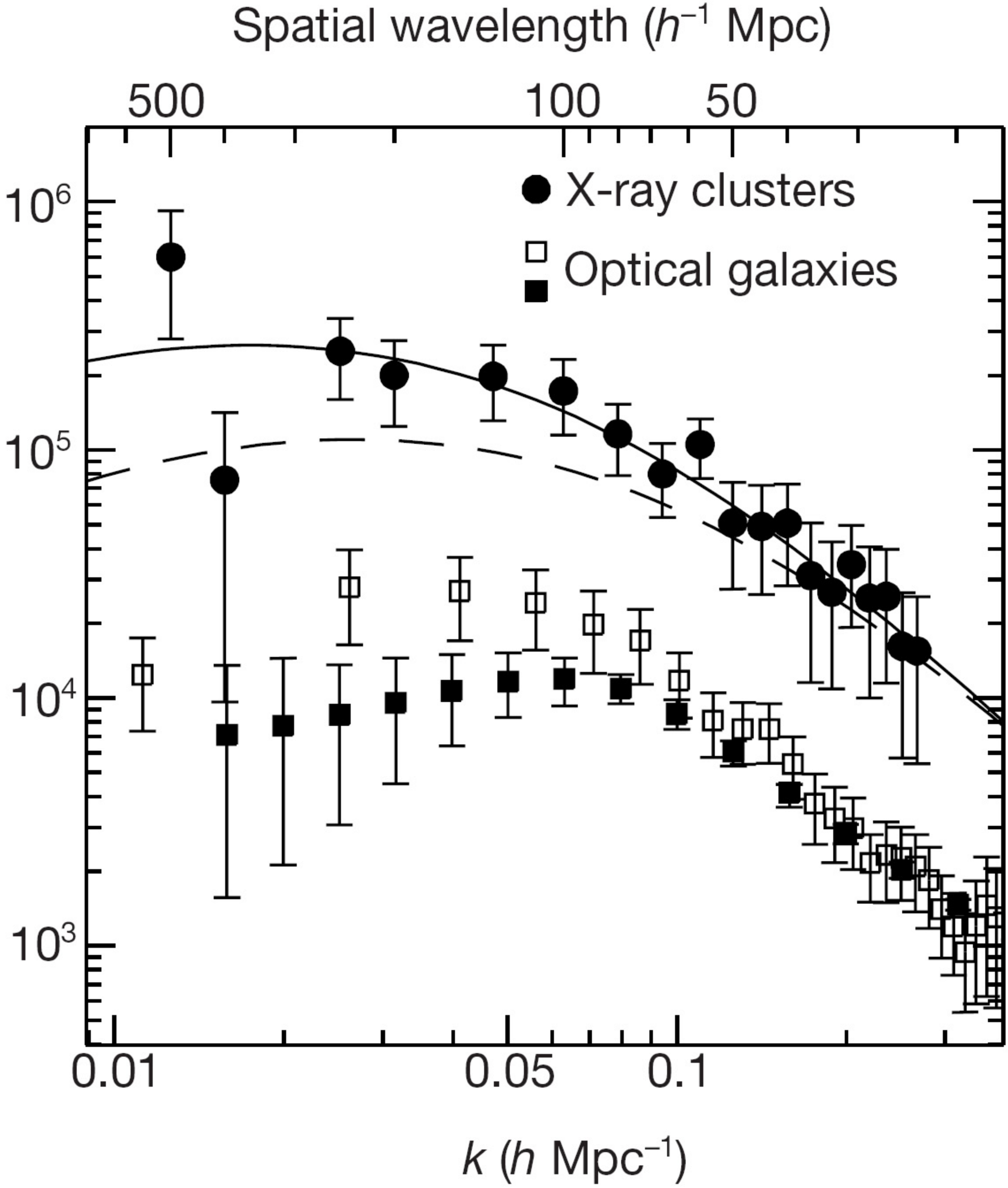
Spatial wavelength (h^{-1} Mpc)
500
100
50
X-ray clusters
Optical galaxies
10^6
10^5
10^4
10^3
$P(k)$ (h^{-3} Mpc^3)
0.01
0.05
0.1
k (h Mpc^{-1})